IEEE Access
Multidisciplinary | Rapid Review | Open Access Journal

Received May 13, 2019, accepted June 6, 2019, date of publication June 12, 2019, date of current version June 27, 2019.

Digital Object Identifier 10.1109/ACCESS.2019.2922294

A Time-Slotted Molecular Communication (TS-MOC): Framework and Time-Slot Errors

ETHUNGSHAN SHITIRI[1], (Member, IEEE), H. BIRKAN YILMAZ[2], (Member, IEEE), AND HO-SHIN CHO[1], (Member, IEEE)

[1]School of Electronics Engineering, Kyungpook National University, Daegu 41556, South Korea
[2]Department of Network Engineering, Polytechnic University of Catalonia, Barcelona 08034, Spain

Corresponding author: Ho-Shin Cho (hscho@ee.knu.ac.kr)

This work was supported by the BK21 PLUS project funded by the Ministry of Education, Korea under Grant 21A20131600011, and in part by the National Research Foundation of Korea (NRF) grant funded by the Korean Government (MSIP) under Grant 2017R1A2B4002622.

ABSTRACT Synchronization is a critical issue in molecular communications (MC). Additionally, the lack of an appropriate time-slotted framework for MC systems hinders the in-depth analysis of desynchronization. Therefore, this paper addresses both issues. First, taking inspiration from oscillators found in nature, we propose a time-slotted framework suitable for MC systems where the time instances of the oscillations demarcate the time-slot boundaries. The use of biological oscillators readily satisfies biocompatibility requirements. We name such system as a time-slotted molecular communication-based (TS-MOC) system. A TS-MOC system will be beneficial to many MC applications, such as when multiple nanomachines have to transmit data simultaneously to a control/sink node or share the channel in a time-division multiplexing manner. Second, oscillation perturbations induce desynchronization — the misalignment of time-slots. Desynchronization combined with large propagation delay results in a time difference between the arrival of a signal and the beginning of a time-slot. This phenomenon is called time-slot error, and it can degrade a system's performance. Therefore, the immediate goal is to mitigate time-slot errors. Depending on the initiation type, we propose two synchronization schemes: sender-initiated time-slot alignment and receiver-initiated time-slot alignment. An analytical model for time-slot error is also derived. Our analysis demonstrates that the proposed schemes are robust and energy-efficient — they achieve relatively low errors indicating robustness and relatively less synthesizing energy costs indicating energy efficiency. Our analysis also highlights the good agreement between the simulations and the analytical model. Finally, in conclusion, we provide brief insights into key open research challenges.

INDEX TERMS Biological oscillators, diffusion, energy, nanonetworks, molecular communication, propagation delay, synchronization, time-slot.

I. INTRODUCTION

Molecular communication (MC) is a new communication paradigm where molecules are used as information carriers [1]. It is one of the promising ways to establish communication within a *nanonetwork* that is the interconnection of tiny functional devices, namely *nanomachines* [2]. Nanomachines are generally characterized by low power, low functionalities, and low processing capabilities. As reviewed in [3], the potential tasks for nanomachines include generating a response (e.g., fluorescence) upon sensing a target (e.g., toxic chemical) or delivering a package (e.g., drug particles) to a target site (e.g., infected area).

Recently, studies on time-slotted communication systems for MC-based nanonetworks (MCN) have begun to emerge [4]–[7]. In it, time is divided into subunits called *time-slots*, where a transmitter nanomachine transmits a signal at the beginning of a time-slot, and the receiver nanomachine expects to receive the signal at an intended time-slot. A crucial question that is commonly overlooked is how to convey the time-slot *boundaries information* (i.e., the beginning and end times of a time-slot) to a nanomachine. We could think of a couple of solutions. The first solution is to embed the information on to the memory. Embedding may require additional memory components, which may increase the cost

The associate editor coordinating the review of this manuscript and approving it for publication was Weisi Guo.

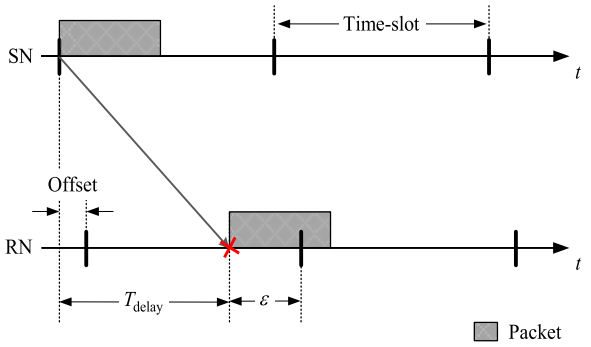

FIGURE 1. Illustration of packet errors in a TDMA system, which are caused by time-slot errors (ε) introduced by the oscillation perturbations and propagation delay (T_{delay}).

and complexity of a nanomachine's hardware. The second solution is to relay the information periodically from an external source. There may be delays in the arrival of the information, or the information may even get corrupted and lost.

A practical approach would be to use the periodic pulses that result from the fluctuations in a molecule's concentration found in biological oscillators [3]. Being periodic means that a pulse of concentration repeats after a fixed duration of time and therefore the boundaries of the time-slots, which are also repetitive, can be marked by the pulse times. Besides periodicity, one other characteristic of biological oscillators is that they are biocompatible — a key requirement for MC systems targeted towards the human body. Biological oscillators may be natural, such as calcium oscillators and circadian oscillators; or synthetic, such as the repressilator [3].

Inspired by the periodic property of biological oscillators, one of the goals of this study is to design a time-slotted framework based on biological oscillators for MC systems. In particular, we wish to position the peaks of the oscillations from biological oscillators as the boundaries of the time-slots. We believe time-slotted systems will be beneficial for MCN applications such as when multiple nanomachines have to transmit data simultaneously to a control/sink node or share the channel in a time-division multiplexing manner. Additionally, the use of biological oscillators readily meets the biocompatibility requirement for MC systems.

In practical scenarios, biological oscillators suffer from oscillation *perturbations* that are caused by noises arising from the stochastic nature of chemical reactions [8], [9]. Such perturbations will lead to misalignment of the pulses of two identical oscillators, meaning they no longer oscillate at the same time instants. In conventional oscillators, such as quartz crystal oscillators, these perturbations are of two kinds: *skews* and *offsets*. Skews refer to the differences in the frequencies of the oscillations while offsets refer to the advance or lag in the oscillations. These type of perturbations are also applicable to biological oscillators. Owing to these perturbations the time-slots will desynchronize and may affect ongoing communication. As an example, Fig. 1 illustrates the time-slot

TABLE 1. List of notations.

Notation	Parameter name
T	oscillation period
T_{slot}	time-slot duration
t_{gi}	guard interval duration
t_{dp}	data part duration
D	diffusion coefficient
d	distance between SN and RN
T_{delay}	propagation delay
S	start time of synchronization
t_{att}	actual transmission time of a signal
t_{arv}	arrival time of a signal
t_{bgn}	beginning time of a time-slot
P_X	time of signal exchanges, X $\in$ (A, B, C, D)
m	number of time-slots between P_C or S and t_{bgn}
ε	time-slot error
G	number of emitted molecules
E_{cost}	energy cost for synthesizing the molecules

desynchronization between a sender nanomachine (SN) and a receiver nanomachine (RN) in a *time-division multiple access* (TDMA) system setting. SN and RN refers to a nanomachine that has to transmit data and a nanomachine that has to receive the data, respectively. Let us say that to transmit a packet, the SN releases a set of molecules and the packet is detected by RN when a threshold is crossed. When the SN, unaware of the time-slot desynchronization, tries to establish communication, the transmitted packet may not arrive at the allocated time duration (i.e., time-slot) resulting in packet errors. The large *propagation delay* — the time taken to cross the threshold — amplifies the problem by further reducing the probability that a packet could arrive at the allocated time-slot. The net effect of the perturbations and the propagation delay creates a difference between the arrival time of a signal and the allocated time-slot. We name this difference in time as the *time-slot error* and denote it by ε (*cf.* Fig. 1).

On that note, we formulate the problem mentioned above as a time-slot synchronization problem as it concerns coordinating the transmitted signal to be received at the beginning of the intended time-slot. Since the perturbations are largely system design related issues, we focus on finding a solution to address the propagation delay aspect of the problem. That brings us to the other goal of this study, that is, to develop methods that can handle time-slot errors. The main objective, here, is to determine a signal's transmission time that combats the variable propagation delay without employing a typical synchronization mechanism of finding the perturbations via time-stamps. Table 1 list the notations frequently used throughout the paper.

We summarize the main contributions of this paper as follows.

- As a first in the literature, we position the peaks of the oscillations from biological oscillators to estimate the boundaries of the time-slots, and name such system as *time-slotted molecular communication* (TS-MOC) system. Furthermore, we investigate a critical problem — time-slot error — that may degrade the performance of a TS-MOC system.
- Using different initiation approaches, we propose two novel energy-efficient time-slot synchronization techniques, namely the *sender-initiated time-slot alignment* (SIT-Algn) and the *receiver-initiated time-slot alignment* (RIT-Algn) technique. Prior works have not addressed the issue of time-slot errors, and that makes our work the first.
- To evaluate the performance of the proposed schemes, we carry out computer simulations concerning oscillation perturbations, guard interval, and the number of emitted molecules. We also investigate the energy spent in the emission of the signal molecules during synchronization. The results highlight the effectiveness of the proposed schemes, such as their ability to handle the perturbations despite not explicitly designed to counteract the perturbations.
- Finally, we derive an analytical model for time-slot errors and demonstrate the agreement between the simulation results and the analytical model.

The remainder of this paper is organized as follows. Section II reviews existing literature on synchronization for MC and outlines the motivation behind time-slot synchronization. Section III presents the system model considered in our study. Section IV describes the design of the TS-MOC system, where we lay down the formal definition of TS-MOC. Additionally, we also present the proposed SIT-Algn and RIT-Algn schemes. This section is followed by Section V where we discuss the simulation settings and the results in detail. Finally, in Section VI we conclude the paper with insights into key open research challenges.

II. RELATED WORKS ON SYNCHRONIZATION

Prior works on synchronization studied various cases of synchronization. We classify and review them categorically based on the approach taken — bio-inspired or traditional.

Taking the bio-inspired approach, an MCN attains synchronization when the concentration of the self-regulating molecules known as autoinducers reaches a certain threshold [10]. Extending the same concept to a cluster of nanomachines, an MCN is able to achieve frequency synchronization [11]. Furthermore, the authors approximate the oscillations as clock signals. In contrast, molecules known as inhibitors are used to achieve different patterns of frequency synchronization [12], [13]. The patterns — in-phase or anti-phase — are influenced by the distance between the nanomachines and the concentration threshold. In [14], phase synchronization was achieved through the exchange of molecular beacon signals. Similarly, extending the concept of the phase-locked loop (PLL) to MC, a molecular PLL was designed to perform phase synchronization [15]. A joint synchronization and detection scheme exploiting the differences in the arrival times between a pilot signal and a data signal was studied in [16].

In the traditional approach, an MCN achieves synchronization through the exchange of time-stamped messages to obtain the time information. The time information may be used to estimate various parameters, such as skew, offset, and propagation delay. In [6], [17]–[19], estimators are derived to obtain the offsets and the skews for Inverse Gaussian channels and Gaussian channels. Similarly, estimators are proposed to achieve symbol synchronization [20]–[22]. A blind synchronization using non-decision directed maximum likelihood estimator is derived in [23].

We note that while these works lay the foundation for synchronization in MC, they do not address time-slot errors. Motivated by the gap in the literature, we draw our attention to time-slot synchronization. Rather than focusing on a common time (namely, time-synchronization, which may be energy inefficient and complex), time-slot synchronization aims to synchronize the time-slots and are, therefore, energy efficient [24]. In that sense, time-slot synchronization is considered a special case of time-synchronization [25].

III. SYSTEM MODEL

We consider two spherical nanomachines separated by a distance, d, between their closest surface points. The transmitter emits a pulse of molecules, G, into the environment. This behavior is similar to the instantaneous release of molecules from a vesicle and the shape of the released molecules is analogous to an impulse signal [12], [26]. The emitted molecules traverse independently in an unbounded three-dimensional environment towards the receiver. Flow is absent in the channel, and therefore the molecules rely solely on Brownian motion for their movements. Consequently, the molecules arrive independently at the receiver and the distribution of their arrival or hitting time is left-skewed with a heavy-right tail, namely Lévy distribution [27]–[29]. The transmitter is considered to be a reflecting transmitter (i.e., hitting molecules are reflected) while the receiver is considered to be a fully-absorbing receiver (i.e., whenever a molecule hits the receiver the molecule is absorbed by the receiver and removed from the environment) [29]–[31]. Furthermore, we assume that a receiver can immediately transmit a signal back to the channel.

Information is encoded using concentration shift keying where a set of molecules are emitted from a transmitter, and the concentration is monitored and thresholded for signal detection at the receiver [32]. In this work, the *propagation delay* is defined as the *peak time of the signal* (i.e., the time it takes to reach the maximum concentration of the arriving molecules at the receiver), which is similarly defined in [29]. (Note that peak time of a signal should not be confused with the peak time of an oscillation. To avoid confusion, we refer to the *peak time of a signal* as the *maximum concentration of the arriving molecules*, wherever necessary.) Owing to the

stochastic motion of the signal molecules, we consider noises in the measured concentration, which leads to variability in the propagation delay. Therefore, we note that the propagation delay is a random variable and is different from the hitting time random variable since it focuses on the probability of absorbing the maximum amount of molecules at a specific time. We also note that there is no firm analytical model of propagation delay that we defined for a molecular diffusion channel, unlike the hitting time distribution in simple scenarios such as point source and spherical absorber. Furthermore, we reiterate that the definition of propagation delay differs from that defined in the literature of timing channels [33 and references therein].

Additionally, we consider the nanomachines to be equipped with identical excitatory biological oscillators [34]. For the sake of brevity, we do not describe the internal workings of the oscillator and direct the readers to the original article [34] and for more background information on oscillators, we direct the readers to the survey article [3 and references therein]. For simplicity, the oscillators have a fixed frequency, i.e., skews are assumed absent. By laying down that assumption, the oscillators will have the same oscillation period for the duration of the study. We note that though the oscillators are free of skews, time-slot errors will persist as it is a function of the offset in addition to the propagation delay. Furthermore, that assumption allows us to study in isolation the effects of the offsets and the propagation delay on the time-slot error. We note that addressing the skew issue is beyond the scope of this study.

IV. TIME-SLOTTED MOLECULAR COMMUNICATION SYSTEM

We name the proposed framework that utilizes biological oscillators to estimate the boundaries of the time-slots as *time-slotted molecular communication* (TS-MOC) system. As might be expected, TS-MOC divides time into time-slots where each time-slot duration has a length equal to integer multiples of the *oscillation period* (duration between the peaks of two consecutive pulses). In each time-slot, a nanomachine may perform simple functions: message transmission, reception, or both; overhead functions such as synchronization; and advanced overhead functions such as channel estimation. We consider TS-MOC to be a generic framework in the sense that one may employ any biological oscillator and in any manner depending on a system's requirements. For example, a nanomachine could obtain the boundary information either from an embedded oscillator, such as the repressilator or from a central oscillator, such as the rhythmic heartbeat. From the perspective of a network topology, the former leads to a distributed topology, while the latter leads to a centralized topology. In this study, we considered the former.

Fig. 2 (top) illustrates the oscillations and the peaks generated by a biological oscillator. The duration T denotes the oscillation period. In Fig. 2 (bottom), we present the proposed framework of a TS-MOC system. Each time-slot boundary

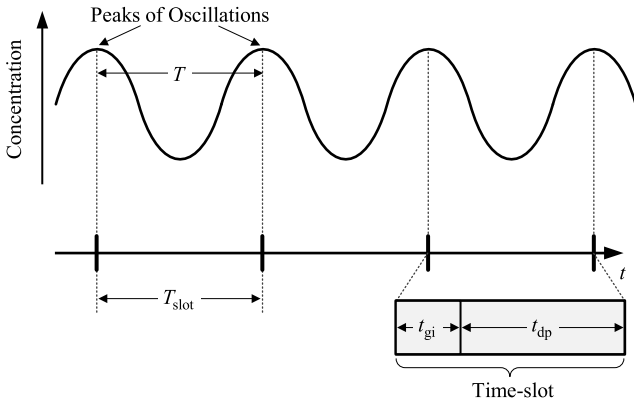

FIGURE 2. Time-slotted Molecular Communication (TS-MOC) framework depicting the mapping between the peaks of the oscillations and the time-slot boundaries (Top), and the internal structure of a single bipartite time-slot consisting of the guard interval part and the data part (Bottom). T, T_{slot}, t_{gi}, and t_{dp} denotes the oscillation period, the durations of the time-slot, guard interval part, and the data part, respectively. Pulses are exaggerated for illustration purposes.

is mapped to the peaks of the oscillation. A unique feature of biological oscillators is the relatively slow oscillation frequencies (up to 500 mHz) compared with quartz crystal oscillators (up to 4 GHz) [3 and references therein]. Therefore, T, which is inversely proportional to the frequency, will be sufficiently large to be considered the time-slot duration, T_{slot}.

Definition 1: TS-MOC is a time-slotted molecular communication system, wherein the beginning and the end of a time-slot is demarcated by the time instants at which the peaks of the oscillations from a biological oscillator occur. □

A single bipartite time-slot is composed of a *guard interval* part and a *data* part (*cf.* Fig. 2). The guard interval part, inserted at the start of the time-slots, act as tolerance against the errors. The data part is used to perform any of the functions mentioned earlier. Therefore, the duration of T_{slot} is the sum of the guard interval duration (t_{gi}) and the data part duration (t_{dp}) given as

$$T_{slot} = t_{gi} + t_{dp}, \quad t_{gi} << t_{dp}. \tag{1}$$

One of the systems where we can implement the TS-MOC framework is a TDMA system. In a TDMA system, a time-slot at the receiver (which could be a central node that gathers data from multiple nodes) needs to be exclusively allocated to a single sender. Intuitively, to use the allocated time-slot efficiently, the message needs to arrive at the beginning of a time-slot. That intuition leads us to establish the following criterion.

Criterion 1: In TS-MOC, the transmission of a signal may not necessarily be at the beginning of a time-slot. However, the reception of the signal must be at the beginning of a time-slot. □

To elaborate further on the importance of criterion 1, we consider the following example as shown in Fig. 3.

Example 1: Suppose, a signal is transmitted by the SN at the beginning of a transmission time-slot, say t_0. The signal

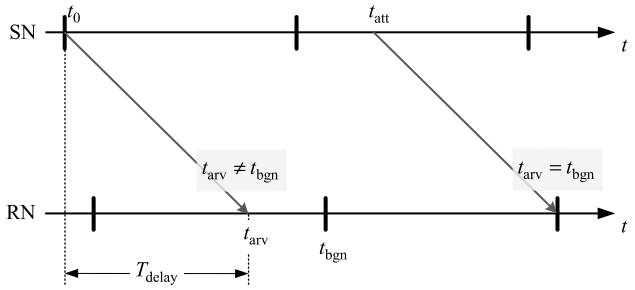

FIGURE 3. Illustration of the scenario described in *Example 1*.

arrives after some delay at the RN at t_{arv} given by

$$t_{arv} = t_0 + T_{delay}, \quad T_{delay} > 0. \tag{2}$$

Let t_{bgn} denote the beginning of a time-slot at which the signal is expected to arrive. From Criterion 1, t_{arv} must be equal to t_{bgn}. Clearly, for $t_{arv} = t_{bgn}$, the transmission time t must take into account the T_{delay}, otherwise time-slot errors (ε) will occur, i.e., $\varepsilon = t_{arv} - t_{bgn} > 0$. We refer to the time instant t_0 that guarantees $t_{arv} = t_{bgn}$ as the *actual transmission time*, denoted by t_{att}, and can be expressed as

$$t_{att} = t_{bgn} - T_{delay}. \tag{3}$$

□

In addition to the importance of criterion 1 that we just described, Criterion 1 may help reduce the influence of the heavy-right tail distribution of the molecules on the subsequent time-slots, which may effectively combat the interferences, such as inter-symbol interferences (ISI). We note that the analysis of ISI is beyond the scope of the paper.

A. SENDER-INITIATED TIME-SLOT ALIGNMENT

To address time-slot errors, through the determination of t_{att}, we develop a novel time-slot synchronization technique, namely, the sender-initiated time-slot alignment (SIT-Algn) technique. SIT-Algn combats the effects of the random propagation delay on t_{arv}. More specifically, without using time-stamps, SIT-Algn estimates T_{delay} and t_{bgn}, which are then used to obtain the t_{att}. T_{delay} will be different for each signal, which we denote as $T^{(1)}_{delay}$, $T^{(2)}_{delay}$, $T^{(3)}_{delay}$, and $T^{(4)}_{delay}$. We note that the numbers in round brackets identify the propagation delays associated with every signal transmission. As we stated earlier and to the best of our knowledge, there is no firm analytical model of the propagation delay (i.e., the distribution of the peak time of a signal) in a molecular diffusion channel. Hence, we adopt an approximated model, where the propagation delay is once estimated, and then all remaining propagation delays are assumed the same as the estimated value.

Note that in naming the proposed scheme, without loss of generality, we prefer the term 'alignment' over 'synchronization' mainly because to attain synchronism the goal of the proposed scheme is to *align* the signal arrival time to the beginning time of a time-slot.

SIT-Algn's operation consists of a series of signal exchanges. As shown in Fig. 4, SIT-Algn begins with the SN transmitting a signal at a time $S = 0\,s$ to the RN. The signal arrives at the RN at $P_A = S + T^{(1)}_{delay}$, where $T^{(1)}_{delay}$ is unknown. On receiving the signal, the RN immediately responds with a signal to the SN, which arrives at the SN at $P_B = P_A + T^{(2)}_{delay}$. SN records P_B. Then using the observed value of P_B, the SN can estimate the propagation delay as

$$\hat{T}_{delay} = \frac{P_B - S}{2}, \tag{4}$$

where $\hat{T}_{delay}$ is the estimated T_{delay}. Meanwhile, soon after RN records P_A, RN performs a second action by transmitting another signal at the time P_C, which is the beginning of the next time-slot following P_A. The signal arrives at the SN at $P_D = P_C + T^{(3)}_{delay}$. Then SN records the arrival time as P_D. Using the information of P_D and $\hat{T}_{delay}$, SN can obtain the time at which the second signal was transmitted, P_C, as

$$\hat{P}_C = P_D - \hat{T}_{delay}. \tag{5}$$

Next, we need to obtain the parameter m, which is the number of time-slots between $\hat{P}_C$ and the t_{bgn} of the time-slot whose beginning we intend to align with the t_{arv}. Then m is given by

$$m = \left\lceil \frac{\hat{P}_C + 2\hat{T}_{delay}}{T_{slot}} \right\rceil, \tag{6}$$

where $\lceil x \rceil$ is the ceiling operator that maps x to the nearest integer greater than or equal to x. The constant 2 denotes the number of propagation delays occurring between $\hat{P}_C$ and t_{bgn}. Recall that $\hat{T}_{delay}$ is an approximation and as such the product of the constant and $\hat{T}_{delay}$ is also an approximation. Then the t_{bgn} of the time-slot at which we intend to align the t_{arv} is given by

$$\hat{t}_{bgn} = \hat{P}_C + mT_{slot}, \tag{7}$$

where $\hat{t}_{bgn}$ is the estimate of t_{bgn}. Substituting (4) and (7) in (3), the t_{att} can be obtained as

$$t_{att} = \hat{t}_{bgn} - \hat{T}_{delay}. \tag{8}$$

By obtaining the t_{att} through (8), the SN can proceed to perform a signal transmission such that the signal will arrive at t_{bgn}. Substituting (4) – (7) in (8) and rearranging in terms of P_D and P_B we obtain

$$t_{att} = S + P_D - P_B + T_{slot}\left\lceil \frac{2P_D + P_B - S}{2T_{slot}} \right\rceil. \tag{9}$$

From (9), we can see that SIT-Algn requires only two recorded observations, i.e., P_B and P_D. Moreover, from (1), it follows that a signal transmitted at t_{att} will arrive after a delay $T^{(4)}_{delay}$ as

$$t_{arv} = t_{att} + T^{(4)}_{delay}. \tag{10}$$

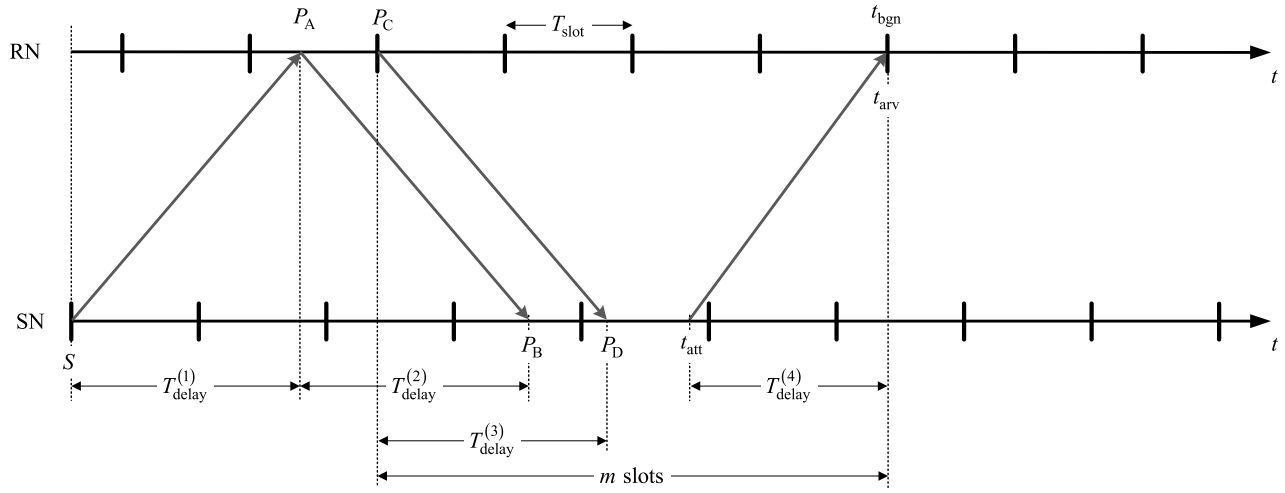

FIGURE 4. Operation of SIT-Algn.

1) ANALYTICAL MODEL OF THE TIME-SLOT ERROR

We shall now derive the analytical model of the time-slot error. Substituting (9) in (10) we get

$$t_{arv} = 2S + P_D - P_B + T_{slot}\left\lceil \frac{2P_D + P_B - S}{2T_{slot}} \right\rceil + T^{(4)}_{delay}. \quad (11)$$

Representing the terms P_B and P_D outside the ceiling operator by their respective propagation delays yields

$$\begin{aligned} t_{arv} &= T^{(3)}_{delay} - T^{(1)}_{delay} - T^{(2)}_{delay} + T^{(4)}_{delay} + t_{bgn} \\ &= \varepsilon + t_{bgn}. \end{aligned} \quad (12)$$

From (12) we can obtain the error as

$$\varepsilon = T^{(3)}_{delay} - T^{(1)}_{delay} - T^{(2)}_{delay} + T^{(4)}_{delay}, \quad (13)$$

where $T^{(1)}_{delay}$, $T^{(2)}_{delay}$, $T^{(3)}_{delay}$, and $T^{(4)}_{delay}$ are independent and identically distributed (i.i.d.) random variables with Normal distribution $N(\mu, \sigma^2)$. For simplicity, we treat propagation delays as Normal distribution as was done in the literature [19]. Due to the property of Normal distribution, ε also follows a Normal distribution with zero mean and $4\sigma^2$ variance [35]. In terms of the expectation operator, we get $E[\varepsilon] = 0$ and $Var[\varepsilon] = E[\varepsilon - \mu]^2 = 4\sigma^2$.

Remark 1: SIT-Algn may be applied to MCNs analogous to sensor networks. For instance, scenarios where a sensor node (i.e., the sender) needs to establish synchronization before it transmits data to the sink (i.e., the receiver). Such cases may arise when a sensor node has critical data for transmission and requires establishing the synchronization immediately. Another plausible scenario is a sensor node requiring synchronization before carrying out a point-to-point communication with a nearby sensor node. □

B. RECEIVER-INITIATED TIME-SLOT ALIGNMENT

Receiver-initiated time-slot alignment (RIT-Algn), much like SIT-Algn, aims to address the time-slot errors through the determination of t_{att}. Additionally, RIT-Algn does not use time-stamps as well. In contrast, however, as the name suggests RIT-Algn is a receiver-initiated scheme and operates differently.

As shown in Fig. 5, the synchronization begins with the RN transmitting a signal at time $S = 0\,s$ to the SN. The signal arrives at the SN at $P_A = S + T^{(1)}_{delay}$. On receiving the signal, the SN records P_A and immediately responds to the RN with a signal, which arrives at RN at $P_B = P_A + T^{(2)}_{delay}$. Then, RN does not need to observe the arrival time and immediately responds to the SN with a signal, which arrives at the SN at $P_C = P_B + T^{(3)}_{delay}$. SN records P_C. Using the observed values of P_A and P_C, the SN can estimate the propagation delay as

$$\hat{T}_{delay} = \frac{P_C - P_A}{2}. \quad (14)$$

On obtaining the information of $\hat{T}_{delay}$, the SN can proceed to obtain the t_{att}. To do so, first, it obtains the parameter m. For RIT-Algn, m is the number of time-slots between S and the t_{bgn} of the time-slot whose beginning we intend to align with the t_{arv}. Then m is given by

$$m = \left\lceil \frac{4\hat{T}_{delay}}{T_{slot}} \right\rceil. \quad (15)$$

Similar to (6), the constant 4 denotes the number of propagation delays occurring between S and t_{bgn}. Here again, we note that the product of the constant and $\hat{T}_{delay}$ is also an approximated value. Let the estimation of S be

$$\hat{S} = P_A - \hat{T}_{delay}. \quad (16)$$

Then the estimate of t_{bgn} is given by

$$\hat{t}_{bgn} = \hat{S} + mT_{slot}. \quad (17)$$

Substituting (14) and (17) in (3), the t_{att} can be obtained as

$$t_{att} = \hat{t}_{bgn} - \hat{T}_{delay}. \quad (18)$$

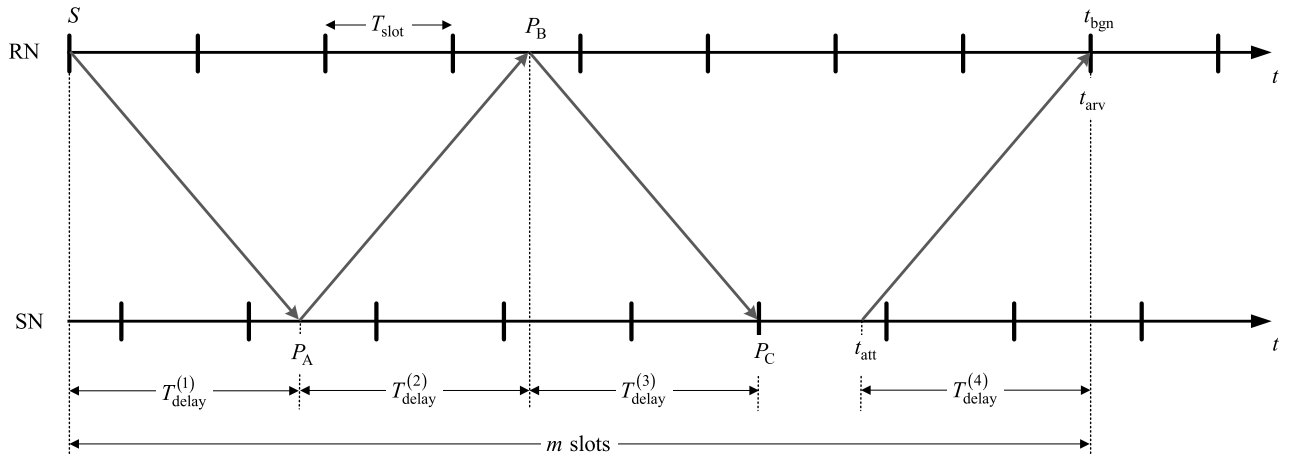

FIGURE 5. Operation of RIT-Algn.

By obtaining the t_{att} through (18), the SN can proceed to perform a signal transmission such that the signal will arrive at the expected t_{bgn}. Substituting (14) – (17) in (18) and rearranging in terms of P_C and P_A yields

$$t_{att} = 2P_A - P_C + T_{slot}\left\lceil \frac{2(P_C - P_A)}{T_{slot}} \right\rceil. \tag{19}$$

From (19), similar to SIT-Algn, we can see that RIT-Algn also requires only two recorded observations, i.e., P_A and P_C. Moreover, from (1)

$$t_{arv} = t_{att} + T^{(4)}_{delay}. \tag{20}$$

By applying the same mathematical treatment discussed in Section IV-A-a, we can easily obtain the same analytical model of the time-slot error as $\varepsilon \sim N(0, 4\sigma^2)$. We note that mapping of the distribution parameters to the physical attributes of a molecular channel and a nanomachine remains as an open research challenge.

Remark 2: RIT-Algn can be applied to MCNs analogous to sensor networks where a sink (i.e., the receiver) needs to establish synchronization before it starts to receive data from a sensor node or multiple sensor nodes (i.e., the sender(s)). □

V. SIMULATION MODEL AND RESULTS

An event-driven simulator was built upon the particle-based MolecUlar CommunicatIoN (MUCIN) simulator in MATLAB software [30]. Through MUCIN, we simulated and recorded the propagation delays experienced by the signals. Then, we built an event-driven simulator that implements the events described in (4) to (10) and (14) to (18). For the detailed working of MUCIN, we direct the readers to the main literature [30]. The radius of the spherical nanomachines are set to $4\mu m$, diffusion coefficient, D, is set at $79.4\,\mu m^2/s$, and data are sampled after every $0.001\,s$. Unless specified otherwise, distance, guard intervals, and the number of emitted molecules are varied as $d = \{5, 6, 7, 8, 9, 10\}\,\mu m$, $t_{gi} = \{0.1, 0.2, 0.3, 0.4, 0.5\}\,s$, and $G = \{1000, 2000, 4000, 6000, 8000\}$ molecules, respectively. T_{slot} is set to $2\,s$, which is reported to be the period of oscillation of a biological oscillator [34]; and in addition, for our system model, this value is sufficiently long to avoid ISI. Except for the values of t_{gi}, which are 5%, 10%, 15%, 20%, and 25% of T_{slot}, the remaining parameters' values are those that are commonly found in the literature [30], [36]. The perturbations are uniformly generated in the range $[-T_{slot}, T_{slot}]\,s$ that covers all possible cases of desynchronization that a time-slot might suffer. This range also includes the worst-case scenario — advanced or lagged by a whole time-slot duration. We note that using a uniform random generator allows us to check the robustness against any values of perturbations.

To evaluate the performances of the schemes, we calculate the time-slot error as

$$\varepsilon = t_{arv} - t_{bgn}. \tag{21}$$

In addition to ε, the mean squared error (MSE) between t_{arv} and t_{bgn} is also used as an evaluation metric. The MSE is expressed as

$$MSE = \frac{1}{M}\sum_{j=1}^{M}\left(t^{(j)}_{arv} - t^{(j)}_{bgn}\right)^2, \tag{22}$$

where $t^{(j)}_{arv}$ and $t^{(j)}_{bgn}$ are the values of t_{arv} and t_{bgn} obtained in the j-th replication, respectively. M is the number of replications, which is set to 10^6. We note that MSE obtained in (22) is the simulation result that corresponds to the analytical result $Var[\varepsilon]\,(= 4\sigma^2)$ obtained using the analytical model of the time-slot error in (13) since $Var[\varepsilon] = E\left[\varepsilon^2\right] - E^2[\varepsilon]$, where $E[\varepsilon] = 0$. We also note that the analytical model derived in (13) applies only to the case without guard intervals.

Another evaluation metric we considered is the *energy cost* — the total energy spent in the emission of the signal molecules used during synchronization. To calculate the energy cost, we use the model of the energy required for

the synthesis and transportation of hexose isomers presented in [37], which is a modified version of the model developed for proteins presented in [38]. Then, the energy cost, E_{cost}, is given by

$$E_{\text{cost}} = nE_{\text{T}}, \tag{23}$$

where E_{T} is the total energy required to synthesize G number of molecules and n is the total number of signaling overheads required to complete synchronization. For the sake of clarity, we reproduce the formulation of E_{T} which is given by [37]

$$E_{\text{T}} = GE_{\text{S}} + \frac{G}{c_{\text{V}}}\left(E_{\text{V}} + E_{\text{C}} + E_{\text{E}}\right), \tag{24}$$

where E_{S} is the synthesizing cost of one hexose molecule calculated from the sum of bond energies (e.g., the enthalpy change), and E_{V} is the vesicle-synthesizing cost having a radius of r_{V}. E_{C} is the cost of intra-cellular transportation having cell radius of r_{unit}, E_{E} is for membrane fusion, and c_{V} is the vesicle capacity, the number of messenger molecules one vesicle can carry, which is related to the radius of messenger molecules r_{m}.

To highlight the effectiveness of the proposed schemes, we compare their performances with an MLE-based synchronization scheme [18]. The rationale for choosing [18] as the comparing scheme is mainly for two reasons. Firstly, for the fact that they also consider clock offsets as the only source of perturbations in the oscillators. Secondly, unlike our approach, they consider time-stamps to perform synchronization. Briefly, the comparing scheme performs N rounds of two-way message exchanges to obtain the time observations and use that information to estimate the offset and the propagation delay. We set $N = 5$, which is a feasible value to find a reasonable estimate of the parameters mentioned above while maintaining a lower energy cost. We note that the transmission time in the comparing scheme is the time within a time-slot immediately after the estimation of the parameters and it is calculated using the estimates of the offset and propagation delay.

In the following sections, we present the performance analysis in terms of ε, MSE, and energy cost. First, we analyze the behavior of ε under different perturbation conditions with a fixed G and without guard interval.

A. ANALYSIS OF $\mathcal{E}$ BEHAVIOR TO PERTURBATIONS

The cumulative distribution function (CDF) of ε with $t_{\text{gi}} = 0\,s$, $d = 5\,\mu m$, and $G = 8000$ molecules is presented in Fig. 6. We reiterate that the value of ε indicates how close t_{arv} is to the t_{bgn}. It can be observed that the proposed schemes have relatively higher convergence rates. The convergence rate is the rate at which the CDF curves converge towards 1. Additionally, we can observe that the proposed schemes have smaller error limits relative to the comparing scheme. Error limits refer to the maximum error value. When perturbations are introduced, we can observe that the performances of the proposed schemes are identical to the case without perturbations and hence the schemes are perturbation-invariant

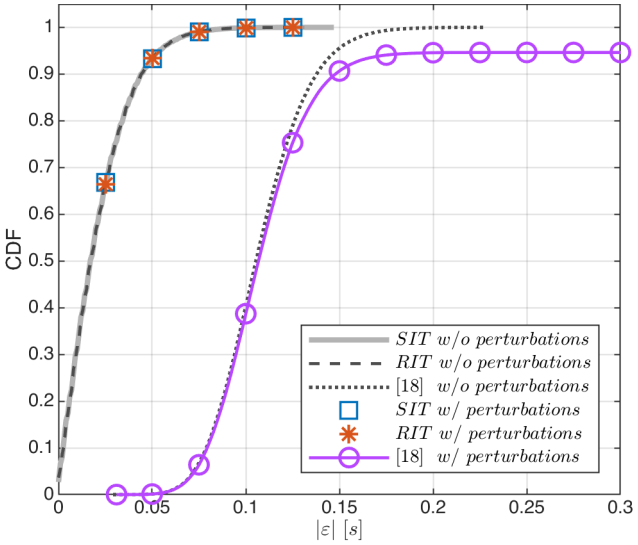

FIGURE 6. CDF with $t_{\text{gi}} = 0\,s$, $d = 5\,\mu m$, and $G = 8000$ molecules.

(*cf.* Fig. 6: the curves without and with perturbations are overlapping with one another). The perturbation-invariant behavior suggests that the initial perturbations do not affect the performance. A similar observation was also reported in [18], which supports our observations and implies that SIT-Algn and RIT-Algn are robust to perturbations. Evidently, that observation makes us believe that while the proposed SIT-Algn and RIT-Algn schemes are not designed to estimate the perturbations and do not utilize time-stamped messages, they can to some degree inherently counteract the perturbations. In contrast, we can observe that the performance of the comparing scheme worsens with the introduction of the perturbations. This relatively poor performance is because the comparing scheme lacks determination of t_{att} whereas the proposed schemes do not.

Additionally, we can observe that the SIT-Algn and RIT-Algn perform identically to each other (*cf.* Fig. 6: overlapped solid, dashed, squared, and asterisked lines). Recall that they are designed with different initiation approaches. This observation implies that while they may differ in the operation mechanism, they aim to reduce time-slot error in the same fashion.

In the next section, we analyze the effects of the guard interval. Unless specified otherwise, hereon, we consider the presence of oscillation perturbations.

B. ANALYSIS OF $\mathcal{E}$ BEHAVIOR TO GUARD INTERVAL

In Fig. 7, the CDF of ε in response to guard interval, i.e., $t_{\text{gi}} > 0\,s$, is plotted and analyzed. We can observe that the performance improves with the insertion of the guard intervals. For instance, for the proposed schemes, when $t_{\text{gi}} = 0.2\,s$, ninety-five percent of the time there are no time-slot errors and when $t_{\text{gi}} = 0.4\,s$, it is approximately a hundred percent. In other words, the errors can be reduced to almost zero percent or to about five percent. Merely doubling the guard

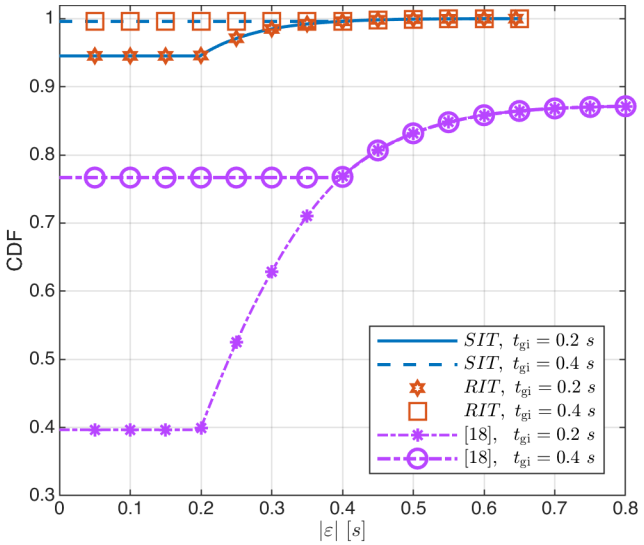

FIGURE 7. CDF for $t_{gi} = \{0.2, 0.4\}\,s$ with $G = 8000$ molecules.

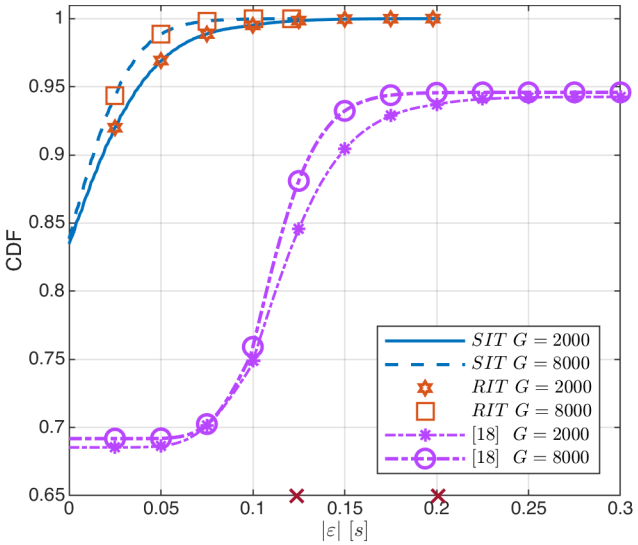

FIGURE 8. CDF for $G = \{2000, 8000\}$ molecules with $d = 5\ \mu m$.

interval yields an improvement of five percent. In contrast, for the comparing scheme, when $t_{gi} = 0.2\,s$, forty percent of the time there are no time-slot errors and when $t_{gi} = 0.4\,s$, it is approximately seventy-five percent, which translates to an improvement of about thirty-five percent. While this margin may seem remarkable, it is negated by the fact that nearly twenty-five to sixty percent of errors remain in the system. Cleary, we can see that the proposed schemes can perform up to twenty-five times better than the comparing scheme. We note that beyond the given t_{gi} values, the straight lines turn into curves that ascend towards 1. These ascending curves reflect the fact that errors higher than the assigned t_{gi} value cannot be mitigated and therefore the curves represent the errors that remain in the system.

In the next section, we analyze the number of emitted molecules per signal transmission on the performances. Unless specified otherwise, hereon, we consider the addition of guard intervals.

C. ANALYSIS OF $\mathcal{E}$ BEHAVIOR TO THE NUMBER OF EMITTED MOLECULES

Fig. 8 plots the CDF of ε in response to different numbers of emitted molecules with $d = 5\ \mu m$. For the proposed schemes, we can observe that the convergence rate improves as the number of emitted molecules increases. The improvement is because increasing the number of emitted molecules reduces noises in the measured concentration. As a result, the variances in the propagation delay are lowered. Moreover, we can observe that the error limits are constrained to $0.12\,s$ and $0.2\,s$ for $G = 8000$ and $G = 2000$, respectively (*cf.* red 'x' markers in Fig. 8). We, therefore, note that in the proposed schemes the time-slot error is a function of the number of emitted molecules. In contrast, the convergence rates and the error limits for the comparing scheme are relatively slow and relatively large, respectively. (Marker for error limit of $2\,s$ is not shown to avoid compression of the x-axis). Although we do not show the error limits of the comparing scheme, we note that they are the same for both cases of the number of emitted molecules. This error limit suggests a plausible correlation between the errors in the comparing scheme and the maximum offset considered in our simulations: $2\,s$. From here, we can infer that the proposed schemes can effectively reduce the error limits to values that are significantly smaller than that of the comparing scheme.

In the next section, we analyze the performance in terms of the MSE against distance, guard interval, and the number of emitted molecules.

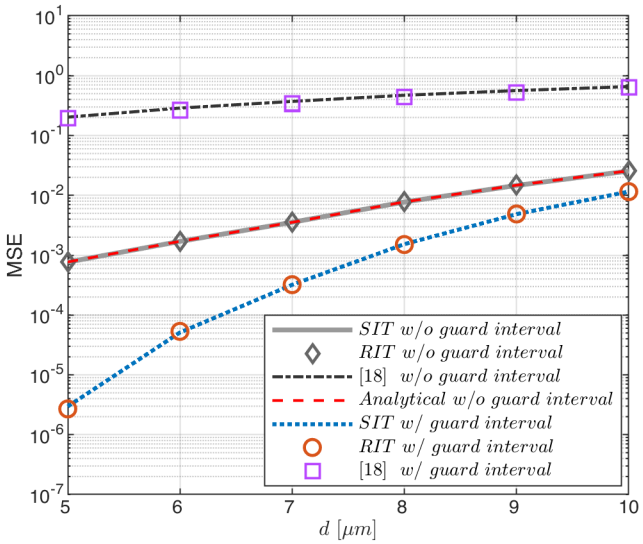

FIGURE 9. MSE versus distance, d, with $G = 8000$ molecules.

TABLE 2. Variance of propagation delay for varying distances and for different number of emitted molecules.

$G = 8000$ *molecules*		$d = 5$ μm	
d $[\mu m]$	σ^2 $[\mu s]$	G $[molecules]$	σ^2 $[\mu s]$
5	192.67	1000	641.65
6	425.33	2000	367.74
7	844.42	4000	258.32
8	1941.19	6000	219.71
9	3693.48	8000	192.67
10	6421.51		

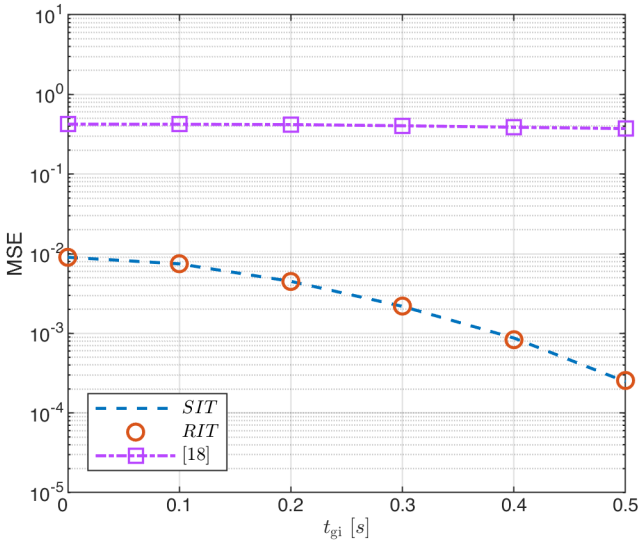

FIGURE 10. MSE versus guard interval, t_{gi}, with $G = 8000$ molecules.

D. ANALYSIS OF MSE

Fig. 9 plots the MSE versus the distance. For the proposed and comparing schemes, each data point represents the data averaged over different guard intervals for each fixed value of distance and with $G = 8000$ molecules. As the analytical result for MSE, we used $Var[\varepsilon] = 4\sigma^2$. Values of σ^2 obtained from MUCIN are listed in Table 2. Regardless of guard intervals, we can observe that MSE is an increasing function of the distance. The increase is expected because larger the distance, lesser number of molecules reach the receiver and that increases the noises in measured concentration. Recall that noises in measured concentration affect the variance of the propagation delay. Thus, the distance also influences the variance of the propagation delay. Without guard intervals, the proposed schemes outperform the comparing scheme by up to three orders of magnitude. Clearly, it is evident that the proposed schemes can effectively handle time-slot errors even in the absence of time-stamps and perturbation knowledge. With guard intervals, we can observe that the proposed schemes outperform the comparing scheme by up to five orders of magnitude. That implies, with guard intervals, the proposed schemes are enhanced by up to two orders of magnitude. Furthermore, we can observe that the

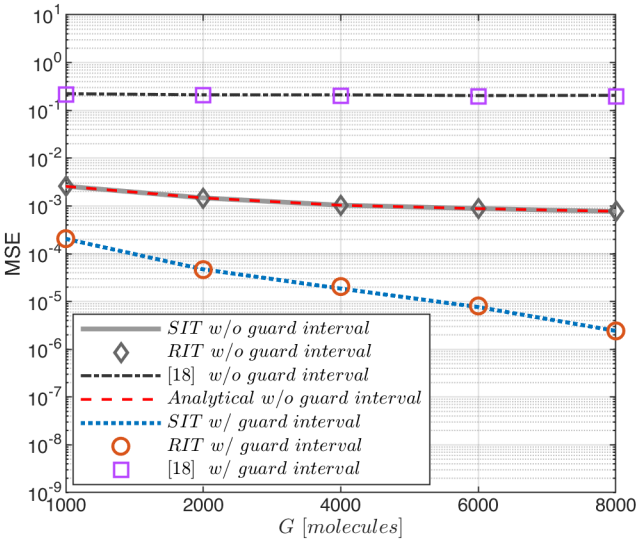

FIGURE 11. MSE versus different number of emitted molecules, G, with $d = 5$ μm.

simulation results (without guard intervals case) agree well with the analytical results. Recall that the analytical model applies only to the case without guard intervals.

To analyze the individual effects of the guard intervals on the performance, we plot Fig. 10. Here, each data point represents the data averaged over varying distances for each fixed value of guard interval and with $G = 8000$ molecules. For the proposed schemes, we can observe that the MSE is a concave downward function of the guard interval. The improvement is expected because guard intervals increase the error tolerance. However, the comparing scheme has negligible improvements in comparison to the proposed schemes. Clearly, this negligible improvement indicates that large durations of guard interval are required for the comparing scheme to compensate for the lack of t_{att}. This method may be inefficient. As we know, the use of large guard interval durations will reduce the duration of the data part, which will negatively affect the throughput of a system. Therefore, as the proposed schemes do not require large durations of the guard interval, we note that they are well suited for TS-MOC systems.

Fig. 11 plots the behavior of the MSE against the number of emitted molecules. Each data point represents the data averaged over different guard intervals for each fixed value of the number of emitted molecules and with $d = 5$ μm. For the proposed schemes, we can observe that the MSE decreases as a function of the number of emitted molecules owing to the decrease in the noises of the measured concentrations. In contrast, we observe that the number of emitted molecules does not bear any significant influence on the comparing scheme. From these observations, we can infer two things. On the one hand, it is evident that increasing the number of emitted molecules enhances the performance of the proposed schemes by up to three orders of magnitude (without guard intervals case). On the other hand, since the

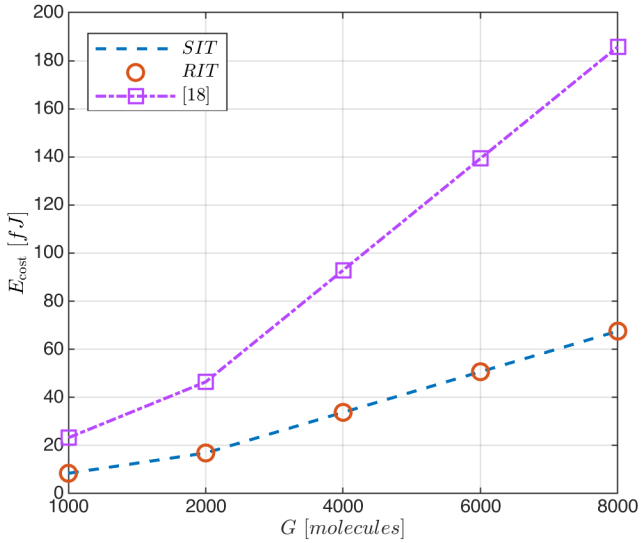

FIGURE 12. Energy costs, E_{cost}, versus different number of emitted molecules, G, with $d = 5\,\mu m$. $1fJ = 10^{-15}J$.

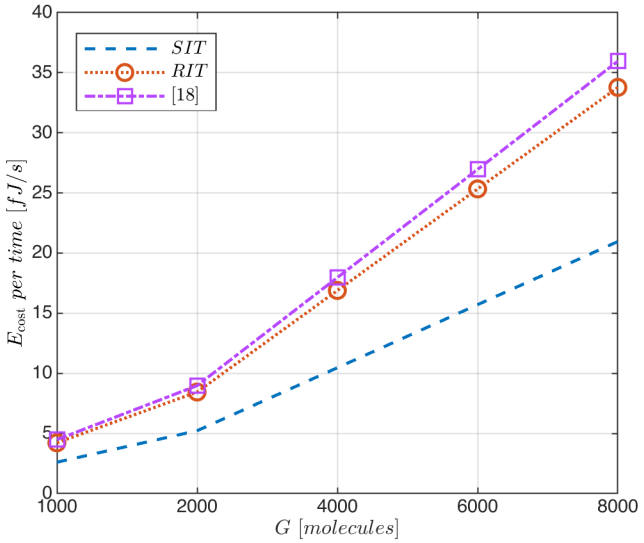

FIGURE 13. Energy costs, E_{cost}, per unit time versus different number of emitted molecules, G, with $d = 5\,\mu m$. $1fJ = 10^{-15}J$.

comparing scheme inherently cannot handle time-slot errors, it is evident that increasing the number of emitted molecules does not enhance its performance whatsoever. With guard intervals, we observe that the performance of the proposed schemes is enhanced even further. In contrast, we observe no significant enhancements for that of the comparing scheme. We note that the overall improvements in terms of the order of magnitude are the same as those observed in Fig. 9. Here again, we observe that the simulation results (without guard intervals case) are in good agreement with the analytical results.

Finally, in the next section, we study the energy spent during synchronization. In particular, we consider the energy spent in synthesizing and transporting the signaling molecules for synchronization.

E. ANALYSIS OF ENERGY COST

We evaluate the energy cost as defined by (22). The value of n is 4 for the proposed schemes, while for the comparing scheme n is $2N+1$, where N is the number of rounds of signal exchanges, each round consists of two signal exchanges, hence the product term $2N$. For fairness, we included an additional signal to the comparing scheme to check the time-slot synchronization accuracy, hence the integer 1. The parameter values of (23) are the same as those found in the literature [37], [38].

As shown in Fig. 12, when the number of emitted molecules increases, E_{cost} grows linearly. We observe that E_{cost} is the same for the proposed schemes as they have the same number of signal exchanges. The E_{cost} of the comparing scheme increases drastically and is almost three times the E_{cost} of the proposed schemes at $G = 8000$. From here, we can clearly see that the proposed schemes require low amounts of energy to perform synchronization.

Comparing the results obtained in Fig. 11 and Fig. 12, we observe that a trade-off exists between E_{cost} and MSE. This trade-off is vividly reflected for the proposed schemes but not for the comparing scheme. To this end, we remark that the schemes which are not inherently designed for TS-MOC systems, and more specifically for handling the time-slot errors, this particular trade-off may be non-existent.

In Fig. 13, we plot the E_{cost} per unit time — energy cost over the total time taken to complete synchronization — versus the number of emitted molecules. Here, we observe that SIT-Algn has a lower E_{cost} per unit time than RIT-Algn. Recall that the proposed schemes spent the same E_{cost}. Thus, we can infer that SIT-Algn takes a longer time to complete synchronization, which we found out to be about $3.2\,s$ and RIT-Algn's is about $2\,s$. In the case of the comparing scheme, the time taken to complete synchronization is larger than the proposed schemes, i.e., about $5.2\,s$. The larger completion time may make one believe that this might result in a lower E_{cost} per unit time. That is not the case. As we just observed that the comparing scheme has a very high E_{cost}, which negates the possibility that the high completion time could effectively lower its E_{cost} per unit time. Therefore, the E_{cost} per unit time of the comparing scheme remains higher than that of the proposed schemes. From here, we can infer that E_{cost} per unit time can be lowered either by having a low E_{cost} or large completion time. However, we caution that it is preferable to have a smaller completion time alongside a lower E_{cost}.

VI. CONCLUSIONS AND DISCUSSIONS

In this paper, we proposed the design of a TS-MOC system based on the peak times of a biological oscillator. We positioned that such a bioinspired approach will greatly benefit applications of MC that are targeted towards the human body. To overcome the time-slot error problem, which was

revealed to be attributed to the combined effects of oscillation perturbations and the variances in the propagation delay, we proposed two time-slot synchronization techniques, namely, SIT-Algn and RIT-Algn. We designed both schemes to obtain the appropriate transmission time of a signal to compensate for the propagation delay, effectively reducing the time-slot errors. Additionally, we derived an analytical model for the mean squared error.

The results show that the proposed schemes achieve time-slot synchronization with relatively lower errors and energy costs, which indicates that the proposed schemes are well suited for TS-MOC systems in terms of robustness and energy-efficiency. It was further shown that that SIT-Algn and RIT-Algn could counteract, to some degree, the perturbations despite not being explicitly designed to handle the perturbations, proving further their effectiveness. A key finding of the study is the tradeoff between the time-slot errors and the energy costs, which can be a useful tool for determining the number of emitted molecules in relation to the permissible errors in a system. Additionally, we observed that the distance parameter has a strong influence on the errors, which can be a useful tool in determining the network coverage area. Although the proposed schemes have identical performances, they are designed for different deployment scenarios. Nonetheless, we observed that SIT-Algn has a longer completion time than RIT-Algn. Finally, we also demonstrated that the simulations are in good agreement with the analytical model.

This study, however, disregards the propagation time of the signal molecules within a nanomachine, such as the time it takes the vesicles to reach the surface of a cell and release the molecules into the environment. For simplicity, this propagation time may be considered to be fixed (and may, therefore, be known to the nanomachines). In reality, the propagation time of the vesicles may be random. The study also disregards the effects of the non-trivial tailing molecules of a signal (or heavy-right tail distribution), which could linger in the subsequent time-slots if the time-slots' duration is not sufficiently long to compensate for the tailing molecules. In such cases, these tailing molecules may interfere with a current signal in a current time-slot and is a pervasive problem faced by MC systems. Additionally, the investigations solely pertain to the case where a receiver is not performing any other communication-related operation, such as receiving a transmission from another nanomachine. Practically, if a receiver is busy, it may not be able to accept an incoming transmission and may lead to collisions. These collisions may affect the throughput of an MCN.

The issues mentioned above remain as open research challenges and addressing them will be vital to the advancement of the research topic under consideration.

REFERENCES

[1] T. Nakano, A. W. Eckford, and T. Haraguchi, *Molecular Communication*, 1st ed. Cambridge, U.K.: Cambridge Univ. Press, 2013.

[2] I. F. Akyildiz, F. Brunetti, and C. Blázquez, "Nanonetworks: A new communication paradigm," *Comput. Netw.*, vol. 52, no. 12, pp. 2260–2279, Aug. 2008.

[3] E. Shitiri, A. V. Vasilakos, and H.-S. Cho, "Biological oscillators in nanonetworks—Opportunities and challenges," *Sensors*, vol. 18, no. 5, p. 1544, May 2018.

[4] T. Nakano, Y. Okaie, and J. Q. Liu, "Channel model and capacity analysis of molecular communication with Brownian motion," *IEEE Commun. Lett.*, vol. 16, no. 6, pp. 797–800, Jun. 2012.

[5] Y. Murin, N. Farsad, M. Chowdhury, and A. Goldsmith, "Time-slotted transmission over molecular timing channels," *Nano Commun. Netw.*, vol. 12, pp. 12–24, Jun. 2017.

[6] B.-K. Hsu, P.-C. Chou, C.-H. Lee, and P.-C. Yeh, "Training-based synchronization for quantity-based modulation in inverse Gaussian channels," in *Proc. IEEE Int. Conf. Commun. (ICC)*, no. 1, May 2017, pp. 1–6.

[7] Z. Cheng, Y. Zhu, K. Chi, Y. Li, and M. Xia, "Capacity analysis for diffusive molecular communication with ISI channel," *Nano Commun. Netw.*, vol. 13, pp. 43–50, Sep. 2017.

[8] M. B. Elowitz, A. J. Levine, E. D. Siggia, and P. S. Swain, "Stochastic gene expression in a single cell," *Science*, vol. 297, no. 5584, pp. 1183–1186, Aug. 2002.

[9] D. Gonze, J. Halloy, and P. Gaspard, "Biochemical clocks and molecular noise: Theoretical study of robustness factors," *J. Chem. Phys.*, vol. 116, no. 24, p. 10997, Jun. 2002.

[10] S. Abadal and I. F. Akyildiz, "Bio-inspired synchronization for nanocommunication networks," in *Proc. IEEE Global Telecommun. Conf. (GLOBECOM)*, Dec. 2011, pp. 1–5.

[11] Ö. U. Akgül and B. Canberk, "An interference-free and simultaneous molecular transmission model for multi-user nanonetworks," *Nano Commun. Netw.*, vol. 5, no. 4, pp. 83–96, Dec. 2014.

[12] M. J. Moore and T. Nakano, "Oscillation and synchronization of molecular machines by the diffusion of inhibitory molecules," *IEEE Trans. Nanotechnol.*, vol. 12, no. 4, pp. 601–608, Jul. 2013.

[13] M. J. Moore and T. Nakano, "Synchronization of inhibitory molecular spike oscillators," in *Bio-Inspired Models of Networks, Information, and Computing Systems* (Lecture Notes of the Institute for Computer Sciences, Social Informatics and Telecommunications Engineering), vol. 103. Berlin, Germany: Springer, 2012, pp. 183–195. [Online]. Available: https://rd.springer.com/chapter/10.1007/978-3-642-32711-7_17

[14] E. Shitiri and H.-S. Cho, "Achieving in-phase synchronization in a diffusion-based nanonetwork with unknown propagation delay," in *Proc. 4th ACM Int. Conf. Nanoscale Comput. Commun. (NanoCom)*, 2017, pp. 1–6.

[15] C. Lo, Y.-J. Liang, and K.-C. Chen, "A phase locked loop for molecular communications and momputations," *IEEE J. Sel. Areas Commun.*, vol. 32, no. 12, pp. 2381–2391, Dec. 2014.

[16] M. Mukherjee, H. B. Yilmaz, B. B. Bhowmik, J. Lloret, and Y. Lv, "Synchronization for diffusion-based molecular communication systems via faster molecules," in *Proc. IEEE Int. Conf. Commun. (ICC)*, Shanghai, China, May 2019. [Online]. Available: https://icc2019.ieee-icc.org/program/symposia#S1569566630

[17] L. Lin, C. Yang, M. Ma, and S. Ma, "Diffusion-based clock synchronization for molecular communication under inverse Gaussian distribution," *IEEE Sensors J.*, vol. 15, no. 9, pp. 4866–4874, Sep. 2015.

[18] L. Lin, C. Yang, and M. Ma, "Maximum-likelihood estimator of clock offset between nanomachines in bionanosensor networks," *Sensors*, vol. 15, no. 12, pp. 30827–30838, Dec. 2015.

[19] L. Lin, C. Yang, M. Ma, S. Ma, and H. Yan, "A clock synchronization method for molecular nanomachines in bionanosensor networks," *IEEE Sensors J.*, vol. 16, no. 19, pp. 7194–7203, Oct. 2016.

[20] V. Jamali, A. Ahmadzadeh, and R. Schober, "Symbol synchronization for diffusion-based molecular communications," *IEEE Trans. Nanobiosci.*, vol. 16, no. 8, pp. 873–887, Dec. 2017.

[21] V. Jamali, A. Ahmadzadeh, and R. Schober, "Symbol synchronization for diffusive molecular communication systems," in *Proc. IEEE Int. Conf. Commun. (ICC)*, May 2017, pp. 1–7.

[22] Z. Luo, L. Lin, W. Guo, S. Wang, F. Liu, and H. Yan, "One symbol blind synchronization in SIMO molecular communication systems," *IEEE Wireless Commun. Lett.*, vol. 7, no. 4, pp. 530–533, Aug. 2018.

[23] H. ShahMohammadian, G. G. Messier, and S. Magierowski, "Blind synchronization in diffusion-based molecular communication channels," *IEEE Commun. Lett.*, vol. 17, no. 11, pp. 2156–2159, Nov. 2013.

[24] B. M. Sadler and A. Swami, "Synchronization in sensor networks: An overview," in *Proc. IEEE Mil. Commun. Conf. (MILCOM)*, Oct. 2007, pp. 1–6.

[25] A. Tyrrell, G. Auer, and C. Bettstetter, "Emergent slot synchronization in wireless networks," *IEEE Trans. Mobile Comput.*, vol. 9, no. 5, pp. 719–732, May 2010.
[26] N. Garralda, I. Llatser, A. Cabellos-Aparicio, E. Alarcón, and M. Pierobon, "Diffusion-based physical channel identification in molecular nanonetworks," *Nano Commun. Netw.*, vol. 2, no. 4, pp. 196–204, Dec. 2011.
[27] B. Tepekule, A. E. Pusane, H. B. Yilmaz, C.-B. Chae, and T. Tugcu, "ISI mitigation techniques in molecular communication," *IEEE Trans. Mol. Biol. Multi-Scale Commun.*, vol. 1, no. 2, pp. 202–216, Jun. 2014.
[28] N. Farsad, W. Guo, C.-B. Chae, and A. Eckford, "Stable distributions as noise models for molecular communication," in *Proc. IEEE Global Commun. Conf. (GLOBECOM)*, Dec. 2015, pp. 1–6.
[29] H. B. Yilmaz, A. C. Heren, T. Tugcu, and C.-B. Chae, "Three-dimensional channel characteristics for molecular communications with an absorbing receiver," *IEEE Commun. Lett.*, vol. 18, no. 6, pp. 929–932, Jun. 2014.
[30] H. B. Yilmaz and C.-B. Chae, "Simulation study of molecular communication systems with an absorbing receiver: Modulation and ISI mitigation techniques," *Simul. Model. Pract. Theory*, vol. 49, pp. 136–150, Dec. 2014.
[31] H. B. Yilmaz, G.-Y. Suk, and C.-B. Chae, "Chemical propagation pattern for molecular communications," *IEEE Wireless Commun. Lett.*, vol. 6, no. 2, pp. 226–229, Apr. 2017.
[32] M. S. Kuran, H. B. Yilmaz, T. Tugcu, and I. F. Akyildiz, "Modulation techniques for communication via diffusion in nanonetworks," in *Proc. IEEE Int. Conf. Commun.*, Jun. 2011, pp. 1–5.
[33] Y. Murin, N. Farsad, M. Chowdhury, and A. Goldsmith, "Communication over diffusion-based molecular timing channels," in *Proc. IEEE Global Commun. Conf. (GLOBECOM)*, Dec. 2016, pp. 1–6.
[34] E. Shitiri and H.-S. Cho, "A biochemical oscillator using excitatory molecules for nanonetworks," *IEEE Trans. Nanobiosci.*, vol. 15, no. 7, pp. 765–774, Oct. 2016.
[35] D. S. Lemons, *An Introduction to Stochastic Processes in Physics*. Baltimore, MD, USA: Johns Hopkins Univ. Press, 2002.
[36] G. Genc, Y. E. Kara, T. Tugcu, and A. E. Pusane, "Reception modeling of sphere-to-sphere molecular communication via diffusion," *Nano Commun. Netw.*, vol. 16, pp. 69–80, Jun. 2018.
[37] N.-R. Kim and C.-B. Chae, "Novel modulation techniques using isomers as messenger molecules for nano communication networks via diffusion," *IEEE J. Sel. Areas Commun.*, vol. 31, no. 12, pp. 847–856, Dec. 2013.
[38] M. S. Kuran, H. B. Yilmaz, T. Tugcu, and B. Özerman, "Energy model for communication via diffusion in nanonetworks," *Nano Commun. Netw.*, vol. 1, no. 2, pp. 86–95, Jun. 2010.

ETHUNGSHAN SHITIRI (S'16-M'18) received the B.E. degree in electronics and communication engineering, the M.Tech. degree in communication systems, and the Ph.D. degree in information and communication engineering from Thanthai Periyar Government Institute of Technology, India, Christ University, India, and from Kyungpook National University, South Korea, in 2010, 2013, and 2018, respectively. He is currently a Postdoctoral Research Fellow with the IDEC Center affiliated to Kyungpook National University, South Korea. His research interests include resource allocation, handshaking protocols, synchronization, and medium access techniques for wireless communication networks – cellular networks, M2M networks, underwater acoustic sensor networks, and molecular communication networks. He was a recipient of the Kyungpook National University Honors Scholarship (KHS). He is a member of KICS.

H. BIRKAN YILMAZ received the B.S. degree in mathematics, in 2002, the M.Sc. and Ph.D. degrees in computer engineering from Bogazici University, in 2006 and 2012, respectively. He worked as a Postdoctoral Researcher with Yonsei Institute of Convergence Technology, Yonsei University, Korea, for four years. He is currently a Postdoctoral Researcher with the Universitat Politecnica de Catalunya, Spain via Beatriu de Pinos Fellowship. He was awarded TUBITAK National Ph.D. Scholarship during his Ph.D. studies and the Marie Sklodowska-Curie Actions Seal of Excellence, in 2016. He was the co-recipient of the Best Demo Award in IEEE INFOCOM (2015) and Best Paper Award in AICT (2010) and ISCC (2012). He is a member of TMD (Turkish Mathematical Society). His research interests include cognitive radio, spectrum sensing, molecular communications, and detection and estimation theory.

HO-SHIN CHO (S'92-M'99) received the B.S., M.S., and Ph.D. degrees in electrical engineering from the Korea Advanced Institute of Science and Technology (KAIST), in 1992, 1994, and 1999, respectively. From 1999 to 2000, he was a Senior Member of the Research Staff with the Electronics and Telecommunications Research Institute (ETRI), where he was involved in developing a base station system for IMT-2000. From 2001 to 2002, he was a Faculty Member with the School of Electronics, Telecommunications, and Computer Engineering, Hankuk Aviation University. In 2003, he joined the Faculty of the School of Electronics Engineering, Kyungpook National University, and currently is a Professor. His current research interests include traffic engineering, radio resource management, and medium access control protocol for wireless communication network, cellular network, underwater communication, and molecular communication. Prof. Cho was awarded the Rising Research Fellowship of NRF in 1998, and is a member of the IEICE, IEEK, KICS, and ASK.